Spectra of the two official GLEs of solar cycle 24

Jorge A. Perez-Peraza [*], Juan C. Márquez-Adame, Rogelio A. Caballero-Lopez,
Roberto R. Manzano Islas

Instituto de Geofísica, Universidad Nacional Autónoma de México, Ciudad Universitaria, 04510 CDMX, Mexico

Abstract

Based on ground-level data and on satellite data we determine in this work the observational spectrum of both, the Ground Level Enhancement of May 17, (2012) the so-called GLE71 and the Ground Level Enhancement of September 10, 2017 (GLE 72). We describe a simplified method to obtain the experimental spectrum at ground level. Data of the GLE71 and GLE72 indicate the presence of two different populations, each one with a different energy spectrum. On the other hand, we explore the kind of phenomena that take place at the source in these two particular events. In contrast with other methods based on the temporal synchronization between electromagnetic emissions of flares and coronal mass ejections (CME), here we develop an alternative option based on the study of the accelerated particles, by adjusting our theoretical spectra to the observational spectra. The main results of this work are the derivation of the source and acceleration parameters involved in the generation process. These results lead us to construct possible scenarios of particle generation in the source for each one of the two studied GLEs.

© 2019 COSPAR. Published by Elsevier Ltd. All rights reserved.

Keywords: Solar cycle 24 - solar flare particles; Ground level enhancements; Source acceleration spectrum

1. Introduction

The implications of the study of Ground Level enhancements of solar particles have been addressed long ago (e.g. Sakurai, 1974, Shea et. al., 1988; Dorman and Venkatesan, 1993; Miroshnichenko and Perez-Peraza, 2008; McCracken et al., 2012; Miroshnichenko, 2014) due to its incidence at the astrophysical scale and the effects on the terrestrial level. In particular, the temporal profile of the particles provides information about the processes of interplanetary transport and the structure of the interplanetary magnetic field, while the energy spectrum provides information regarding the phenomena at the source, particularly in the acceleration process(es). As it was shown by Pérez-Peraza et al. (1985), at least for protons of $E < 480$ MeV

the modulation of the fluxes may be relatively important for some events. On the other hand, in Miroshnichenko (2001), (beginning of section 1 at the end of section 8.1, there are some arguments (e.g. Reames, 1999) where the author suggested that Electric fields of the solar wind, in the first approximation, can be neglected and collisions of Solar Cosmic Rays with particles of the solar wind are insignificant. In Section 8.3.2 of the same book, there is an interesting discussion about the shift in the transport paradigm. At any event, transport theory is a complicated matter, out of the scope of this work.

Generally, synchronization of time between the electromagnetic emissions of solar flares with those of solar energy particles and coronal mass ejections (CME) is the method used to explore the physical conditions and processes that take place at the sources of solar particle generation (e.g., Gopalswamy et al., 2013). Alternatively, the comparison of the observational and the theoretical energy

spectra leads us to make inferences regarding the phenomena at the source, particularly the physical parameters of the source and the type of acceleration mechanisms involved in the phenomenon (e.g., Gallegos-Cruz and Perez- Peraza, 1995; Perez-Peraza et al., 2009, 2018). At present, it is generally envisaged that the particles are accelerated due to two types of processes of a different nature: a deterministic and a stochastic acceleration processes. Among the more plausible proposals is the magnetic reconnection of the field lines in the flare body, or in its surroundings, and on the other hand in the turbulence of the flare plasma, or behind the shock waves associated with the coronal mass ejection (ME). Besides, it was observed that some GLE present two acceleration phases: a Prompt Component (PC) and a Delayed Component (DC), as was evidenced long ago by the group of the Polar Geophysical Institute of Apatity, Russia, (e.g. Vashenyuk et al., 1993, 1994, 2011) and recently designated as early and late phases of Mishev et al. (2014), or even as episodes (Plainaki et al., 2014). For the particular case of the Ground Level Enhancement of May 17, other authors (e.g. Kuwabara, et al., 2012, 2013; Berrilli et al., 2014) have also indicated two possible populations, during the GLE71, supporting the presence of a PC and a DC.

By comparing theoretical and observational spectra we attempt in this work to develop scenarios that can provide us with some insights of the phenomenon of particle acceleration during solar flares. It should be emphasized that our main goal is the study of the particle spectrum at the source level; therefore, we do not deal here with processes of particle propagation. Studies of effects of his kind on energy spectra have been done since many decades ago by a quite number of groups (Schlickeiser, 1989, Smart and Shea, 1993, Miroshnichenko, 2014). In fact, since we are dealing with highly relativistic energy protons able to penetrate the magnetosphere, it is expected that interplanetary transport does not significantly alter the source spectrum of most of Ground Level Enhancements (GLEs). We will discuss later the case of satellite data of energies lower than 100 MeV.

Let us remember here that (GLEs) are events observed by detectors on the earth's surface when there is an abrupt increase in the cosmic particle count. The scientific international community recognizes at least 72 GLEs events from February 28, 1942, to September 10, 2017; currently, there is a worldwide network of neutron monitors at the earth level (NMDB, http://www.nmdb.eu). It has been well known for approximately the last seven decades that GLEs are characterized by a rapid increase of their maximum intensity, taking place within a few minutes, with decay being much slower than the increase; flows are highly anisotropic at the beginning and sometimes throughout the GLE (e.g. Moraal and Caballero-Lopez, 2014). The energy spectrum is softer than that of galactic cosmic radiation, and as the event progresses, it softens. The first four figures show the time profiles of both events being considered (NMDB and satellites data).

2. Data

There is a debate about which stations have registered the GLE of May 17, 2012, and given the smallness of the event at Ground level, however, according several works as for instance those of Poluianov et al. (2017) and Shea et al. (1985), there exist a standardized format for determining cosmic ray ground-level event data. On this basis, we claim that only nine NM stations have discernibly recorded this GLE as is shown in Fig. 1, (from the NMDB). However, based on to the arguments that we will mention later, we reduce our study to two stations, SOPO and SOPB, assuming that the spectrum derived using these two high altitude polar neutron monitors give a reasonable description of the energetic flux that reach the earth ground level.

2.1. GLE of May 17, 2012

This event took place due to a medium intensity solar flare (1F/M5.1, N12W83) and a high-speed CME (1582 km s^{-1}). Many researchers were involved in the study of the different characteristics of this event and its mother solar flare (e.g., Gopalswamy et al., 2013; Li et al., 2013; Balabin et al., 2013; Augusto et al., 2013; Papaioannou et al., 2014, Kuwabara et al., 2013) and so on.

High energy solar protons during this event were recorded not only by high latitude Neutron Monitor stations but also by several spacecraft close to Earth: WIND, GOES, ALTEA and ACE, Berrilli et al. (2014), and some ground-based neutron monitors. The event was quite small, highly anisotropic and was only observed at high latitudes and at a few stations at lower latitudes with a geomagnetic cutoff <3 GV. The maximum increase was 24% according to *one minute* (NMDB) was recorded in the South Pole stations, Fig. 1.

One of the interesting features about the acceleration of solar protons is to compare the behavior of the energy spectrum of low energy protons with that of relativistic protons that reach ground level. Such behavior may give some insights regarding whether the low and the high energy populations proceed from the same, or, different sources.

In the case of the GLE71, the time profile of low energy protons was given in terms of differential flux by Li et al. (2013) based on GOES-13 data (their Fig. 3). To obtain the spectrum value at the four different energies, we use the Time of Maximum (TOM) flux (Forman et al., 1986; Li et al., 2013); Fig. 2: illustrates that for 30.6 MeV, the differential flow becomes ≈7.9 protons/(cm^2 s sr MeV), for 63.1 MeV the differential flow becomes ≈2.0 protons/ (cm^2 s sr MeV), for 165 MeV the differential flow becomes ≈0.18 protons/(cm^2 s sr MeV) and for 433 MeV the differential flow becomes ≈0.058 protons/(cm^2 s sr MeV). The corresponding spectra values obtained in this way are shown in the section of *Results*.
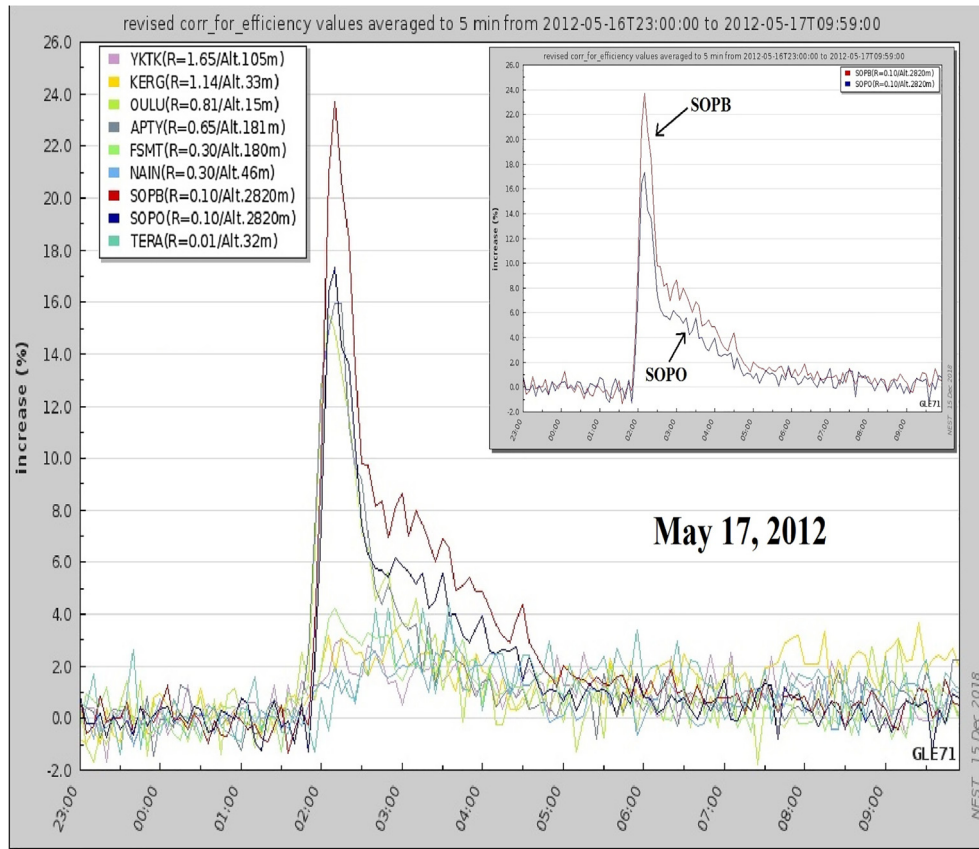
Fig. 1. Increase of the proton flux of 9 stations (NMDB) including SOPO and SOPB during the GLE of May 17, 2012.
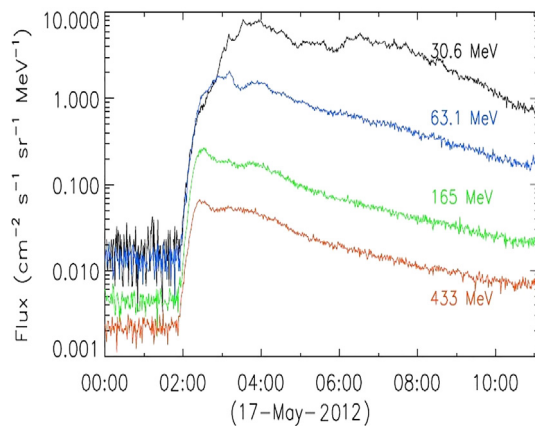

Fig. 2. Differential flux of low energy solar protons as seen by the **GOES-13** satellite on May 17, 2012 during the GLE 71 (Fig. 3 in Li et al., 2013).

2.2. GLE of september 10, 2017

It has been globally disseminated that at the beginning of September 2017 there was a period of extreme solar activity, precisely at the minimum of the solar cycle 24, in the Active Region AR2673 which produced four powerful class X flares, including the strongest flare of the Solar Cycle 24 (X9.3, S08W83) on September 6, 2017. This was the one that produced intensive solar-terrestrial disturbances including a severe geomagnetic storm on September 07 and 08. The corresponding solar activity center also included the second strongest flare (X8.2) of Cycle 24, on September 10, 2017, when the GLE was generated (Augusto et al., 2018; Zhao et al., 2018; Gopalswamy et al., 2018, Cohen and Mewaldt, 2018). The event was observed mainly in high-latitudes (NM) neutron monitors and stations in lower latitudes with a geomagnetic cut <4 GV. It was also a low intensity and highly anisotropic event: the increase at SOPB was ~8% according to *one minute* NMDB data was recorded at the South Pole station, Fig. 3.

In the next section, we derive the energy spectrum at the ground level of this event; we are able to obtain a comparative frame by using the spectrum at low energies from the time profiles in units of differential flux, taken from: https://www.swpc.noaa.gov/products/goes-proton-flux (Fig. 4). As in the case of the GLE 71 we take the flux for four different energies at the Time of Maximum flux (TOM) (Forman et al., 1986): for 7.5 MeV, the differential flow becomes ≈44.6 protons/(cm^2 s sr MeV), for 20 MeV, the differential flow becomes ≈70 protons/(cm^2 s sr MeV), for 40 MeV, the differential flow becomes ≈7 protons/(cm^2 s sr MeV), and for 75 MeV the differential flow becomes ≈2.0 protons/(cm^2 s sr MeV). The corresponding
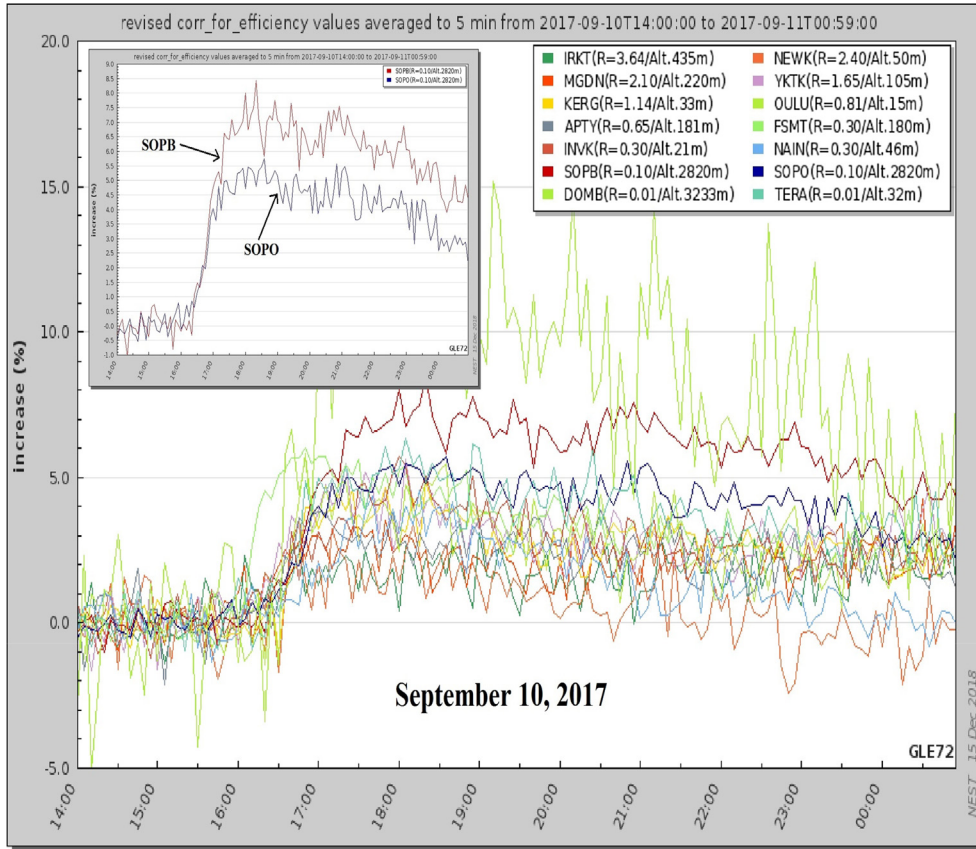
Fig. 3. Increase of the proton flux of 14 stations (NMDB) including SOPO and SOPB during the GLE of September 10, 2017.
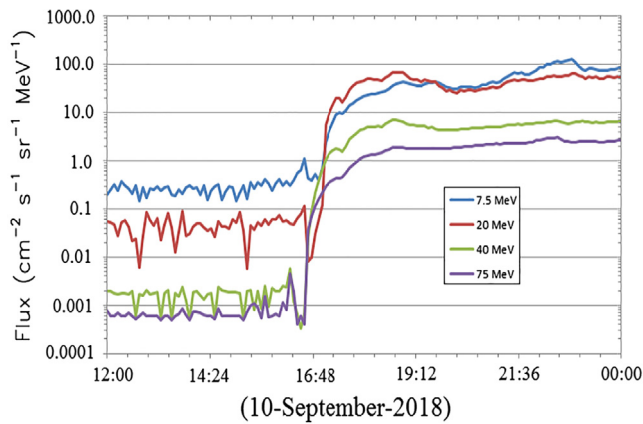

Fig. 4. Differential flux of low energy solar protons as seen by the GOES-13 satellite on September 10, 2017 during the GLE 72. These profiles, in units of differential flux, were obtained from: https://www.swpc.noaa.gov/products/goes-proton-flux.

spectra values obtained in this way are shown in the section of *Results*.

3. Analysis of the cosmic ray spectrum

The counting rate N of a neutron monitor at cutoff rigidity P_c and atmospheric depth x is calculated from the following equation:

$$N(P_c, x) = \int_{P_c}^{\infty} S(P, x) J(P) dp \tag{1}$$

Here, $S(P, x)$ is the atmospheric yield function given in Caballero-Lopez and Moraal (2012) and $J(P)$ is the primary cosmic-ray spectrum at the top of the atmosphere. For the solar cosmic rays, the counting rate, N_s, is usually assumed as a power-law spectrum of the form $J = J_0 P^{-\gamma}$ at the top of the earth's atmosphere. The fractional increase, $\delta N/N$, is given by the ratio N_s/N_g, where N_s and N_g are the counting rates due to solar and galactic cosmic rays, respectively. Pc is the well-known geomagnetic threshold (cutoff rigidity), which determine the minimum energy for cosmic rays reaching the top of the atmosphere at the neutron monitor location (Smart and Shea, 2005).

In this work, we analyze both GLEs based on data from two neutron monitors at South Pole station. They are SOPO NM which is a standard 3NM64 neutron monitor and SOPB NM, a lead-free neutron monitor (LFNM), both located at an altitude of 2820 m a.s.l. with a cutoff rigidity of about 0.1 GV (see, for instance, Oh et al., 2012).

One of the most distinctive features of a GLE is its anisotropy. Therefore, if one compares the increases observed by different neutron monitors, the anisotropy must first be subtracted before spectral information is inferred. With this in mind, several techniques have been used (e.g. DeKoning 1994; Bieber et al., 2002; Ruffolo et al., 2006;

and references therein). Moraal and Caballero-Lopez (2014) and Caballero-Lopez and Moraal (2016) have used the method proposed by Stoker (1985) and used in many works by the University of Delaware group (see for instance, Bieber and Evenson 1991; Oh et al., 2012; Bieber et al., 2013) to minimize the effect of the anisotropy from the spectral sensitivity. This method analyzes the ratio of increases in two neutron monitors with different rigidity response functions, but in the same location. This scenario eliminates the uncertainties due to different atmospheric pressures, temperature and other environmental conditions. Therefore, the method is much more sensitive to small anisotropies. In this work, we will use this technique based on reducing the effects of anisotropy by analyzing the ratio of increase in two neutron monitors, with different response functions, but in the same location. Specifically, we will use the information from the pair of neutron monitors of the South Pole station: SOPO (NM64) and SOPB (LFNM). It should be mentioned that another two pairs of neutron monitors at the same location are in SANAE and DOMC stations.

According to Eq. (6) of Caballero-Lopez and Moraal (2016), the ratio of the fractional increases, observed by these two neutron monitors at the South Pole station, can be written as follows:

$$\frac{(\delta N/N)_{LFNM}}{(\delta N/N)_{NM64}} = \left(\frac{N_g^{NM64}}{N_g^{LFNM}}\right)\frac{\int_{P_c}^{\infty} S_{LFNM}(P,x)P^{-\gamma}dP}{\int_{P_c}^{\infty} S_{NM64}(P,x)P^{-\gamma}dP} = f(\gamma, P_c)$$

(2)

Yield functions in this expression, S_{NM64} and S_{LFNM}, are from Caballero-Lopez and Moraal (2012) and Moraal and Caballero-Lopez (2014), respectively. Eq. (2) means that the spectral index can be calculated from a ratio that is independent of the direction of arrival of particles. We want to emphasize that this technique has been wild used by several authors to estimate the spectrum of solar cosmic rays during a GLE. Caballero-Lopez and Moraal (2012) yield function properly reproduces the neutron monitor counting rate and is in good agreement with other yields obtained from Monte Carlo simulations (see their comparison in Caballero-Lopez, 2016).

Table 1 shows the results of applying Eq. (2) to the observed ratio at South Pole station, during GLE 71 and GLE 72. In our analysis, we have used 15 min moving averages of the data shown in Fig. 1 for SOPO and SOPB. Fig. 5 shows the spectral index as a function of time for both GLEs.

4. The observational solar particle spectra

Regarding the obtained values of (γ), it can be appreciated that in both GLEs there is no definite tendency of the value as time elapses, which leads us to consider that there are two different acceleration phases in both GLEs, a first one designated as the Prompt Component (PC) and a second one namely the Delayed Component (DC).

We must notice that if we want the flux (J_E) respect to proton kinetic energy (E) in units of GeV^{-1} m^{-2} s^{-1} sr^{-1}, then we must multiply the flux respect to rigidity in units of GV^{-1} m^{-2} s^{-1} sr^{-1} by β^{-1} (where β is the ratio of

Table 1
Spectrum parameters at Ground Level.

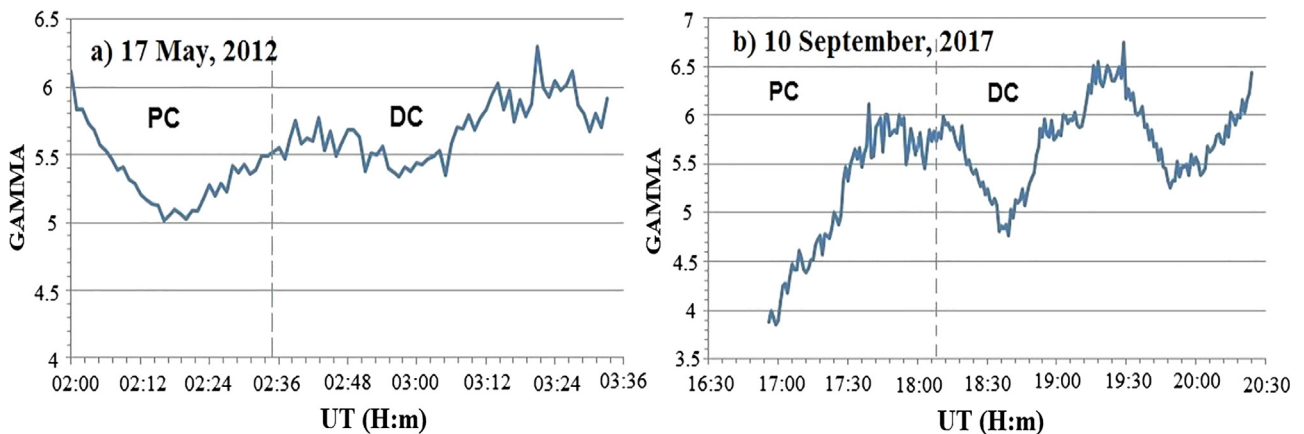| Data GLE	UT	Stage	J_0 (Proton/GV m^2 sr s)	Gamma (γ)
17-may-12	02:00–02:30	PC	3.80 E+04	5.3
17-may-12	02:31–03:30	DC	2.39 E+04	5.6
10-sep-17	16–56-18:14	PC	1.43 E+04	5.2
10-sep-17	18:15–20:24	DC	1.85 E+04	5.7

Fig. 5. Time series of the 15 min simple moving average of the parameter gamma.

particle speed to speed of light). Therefore, we should use the following expression:

$$J_E(E) = 10^{-7} J_0 \frac{E + E_0}{\sqrt{E(E + 2E_0)}} \left(\frac{\sqrt{E(E + 2E_0)}}{1000} \right)^{-\gamma} \quad (3)$$

where J_0 is the flux respect to rigidity for 1 GV protons (and shown in column 4 of Table 1), E is in MeV, $E_0 = 938$ MeV and J_E is in units of MeV^{-1} cm^{-2} s^{-1} sr^{-1}. To deduce expression (3), we used the relationship between rigidity, P, proton kinetic energy, E, and as indicated in the next expression:

$$P = \sqrt{E(E + 2E_0)} = \beta(E + E_0) \quad (4)$$

From the data obtained in the Table 1 we have constructed the following energy spectra at ground level. For both events we have derived the spectrum J_{sp} (P, t) $= J_0 P^{-\gamma}$ by the method mentioned above of Caballero-Lopez and Moraal (2016). The results are illustrated in Fig. 6.

In Perez-Peraza et al. (2018), the observational spectra given by different authors (Balabin et al., 2015; Kuwabara et al., 2012; Plainaki et al., 2014; Mishev et al., 2014) were exhaustively studied for the GLE71. The authors shown in Fig. 7 published their spectra in terms of flux. The satellite data used by Matthiä et al. (2018), is shown by us in Fig. 7c and d. Relative to the GLE71 (Fig. 7a and b) it should be noted that our spectrum is included in the order of magnitude of that of other authors, who used a large number of stations; this may be understood from the use of many response functions, and that each author resorted to a different yield function. Although in the case of Kuwabara et al. (2012), the stations are the same as ours, they do not use response and yield functions as those derived Caballero-Lopez and Moraal (2012). For the GLE72 our spectrum is very close to that

of Matthiä et al. (2018), specifically at satellite energies, which correspond to the data used by these authors. Regarding Mishev et al. (2018) it can be seen in Fig. 7c that the PC of the three spectra are of the same order, while the DC differs, particularly at low energies (Fig. 7d).

5. The source spectrum

The study of the energetic distribution of non-thermal particles is a fundamental problem in Cosmic Ray Astrophysics. The particle energy spectrum contains the information about particle generation processes, the source location, and physical conditions therein. To determine particle spectra at the level of their sources several methods have been worked out; by demodulation of the observational data back to the source, taking into account the processes that may take place during the interplanetary transport (Perez-Peraza et al., 1985, Alvarez et al., 1986), or alternatively, by inferring the particle source spectrum from the deconvolution of the non-thermal electromagnetic emissions produced by the interaction of the accelerated particles, with the local matter and electromagnetic fields. Both mentioned methods lead to a source spectrum that may be fitted by an exponential or inverse power law in energy, which by itself does not contain great information about the source phenomenology and physical conditions, but this must be inferred from additional theoretical work.

For this later goal, usually two different approaches have been worked out in the literature.; the first one consists in developing an acceleration mechanism for the particles to gain energy· in the proposed electromagnetic field configuration and deriving the corresponding energy distribution predicted by the mechanism (Perez-Peraza et al., 1978; Gallegos and Perez-Peraza, 1987; Gallegos et al., 1993; Perez-Peraza et al., 1993) and on the other hand a more general method consists in solving a
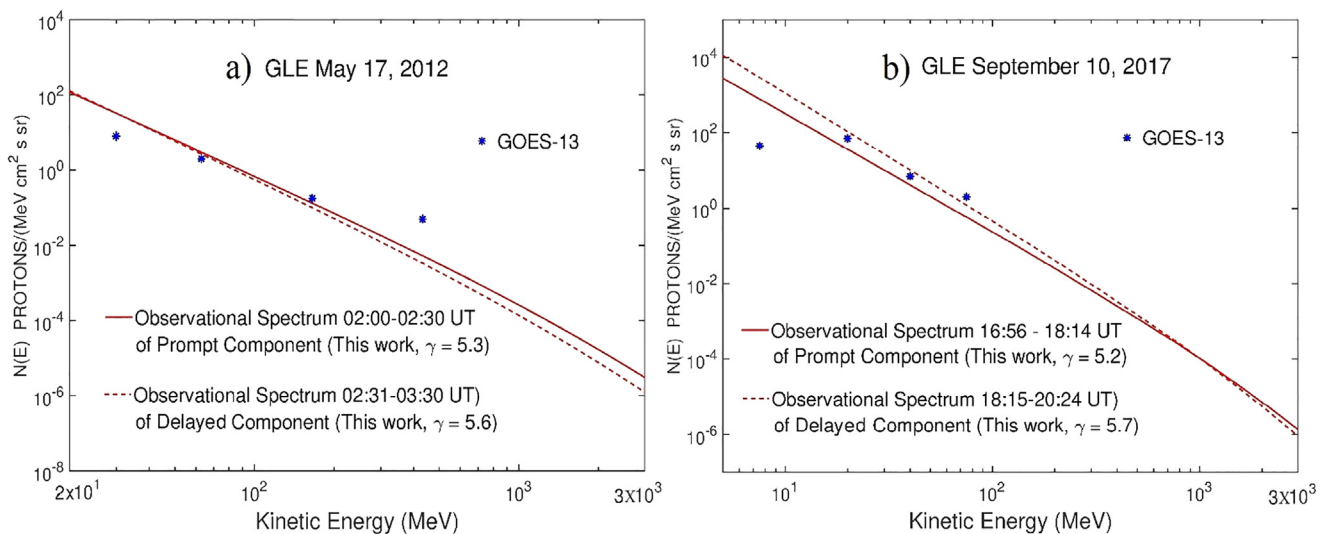

Fig. 6. Observational spectra (Prompt Component and Delayed Component) obtained in this work for the GLE of May 17, 2012, Fig. (a), and for the GLE of September 10, 2017, Fig. (b).
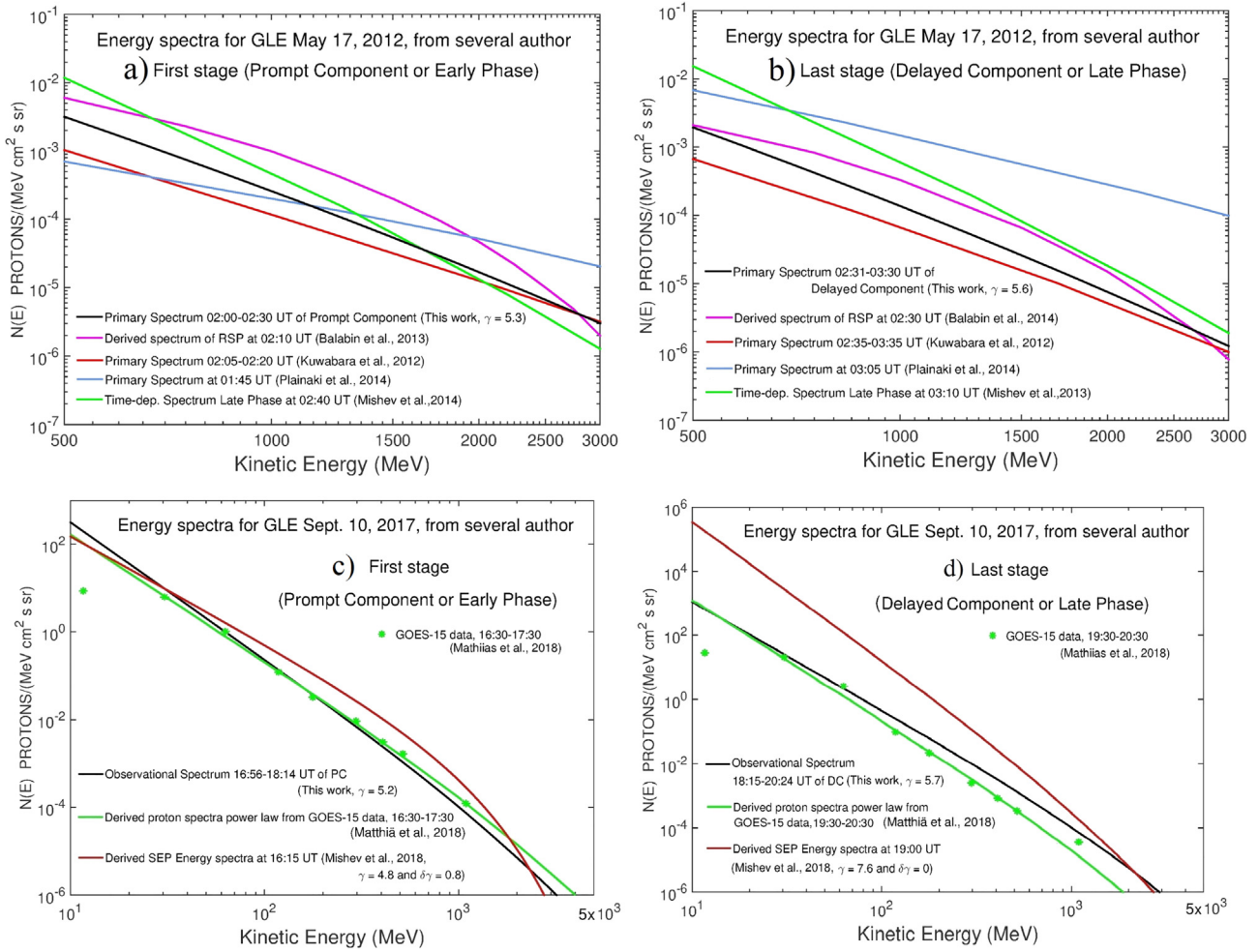
Fig. 7. Energy spectrum derived in this work (in black), as compared with the spectra of other authors.

Fokker-Planc Type equation of continuity in the energy space, Perez-Peraza and Gallegos (1987), Perez-Peraza and Gallegos-Cruz (1994) and Gallegos-Cruz and Perez-Peraza (1995), for several types of plasma turbulence and including adiabatic energy losses (Perez-Peraza et al., 2009). Those works have been summarized in the Appendix of the present work.

To infer about the physical parameters of the source and the different acceleration mechanisms involved in the GLE phenomenon, for both events, we compared the obtained observational energy spectra in this work (Figs. 6 and 7) with the theoretical energy spectra. In Perez-Peraza et al. (2018) an exhaustive study of the source spectra of the GLE71 has been done by means of the comparison of the theoretical source spectra with the experimental spectra, that several authors had published up to the end of 2017. Basically, we have dealt with stochastic acceleration, either in its time-dependent or steady state approaches. As an injection process, we are considering two options: pre-acceleration by monoenergetic flux of protons and reconnection in a Magnetic Neutral Current Sheet (MNCS) typical of flare plasma regions (Perez-Peraza et al., 1977).

6. Results

The comparison of the theoretical and experimental spectra is shown below: Figs. 8 and 9 was done on basis of the theoretical energy spectra, obtained by Gallegos-Cruz and Perez-Peraza (1995), Perez-Peraza et al. (2009), and summarized in the *Appendix*. To determine the physical parameters prevailing at the source, as well as the acceleration and deceleration from adiabatic cooling during particle generation in the two GLEs under study we employed several sets of parameters that susceptibly prevail in the sources of solar particles (e. g., Miroshnichenco and Perez-Peraza, 2008). The meaning of the symbols is described in the *Appendix*.

It should be observed in Fig. 6 that our spectra are quite close to the satellite data of GOES-13. It should also be noted in Fig. 7c and d that most of spectra are close to the data of GOES-15.

Fig. 8a and b show the fitting of the equations, appearing in the works indicated just above, to our observational Prompt and Delayed spectra illustrated in Fig. 6a. The obtained source and acceleration parameters for both components are indicated in the body of Figures.
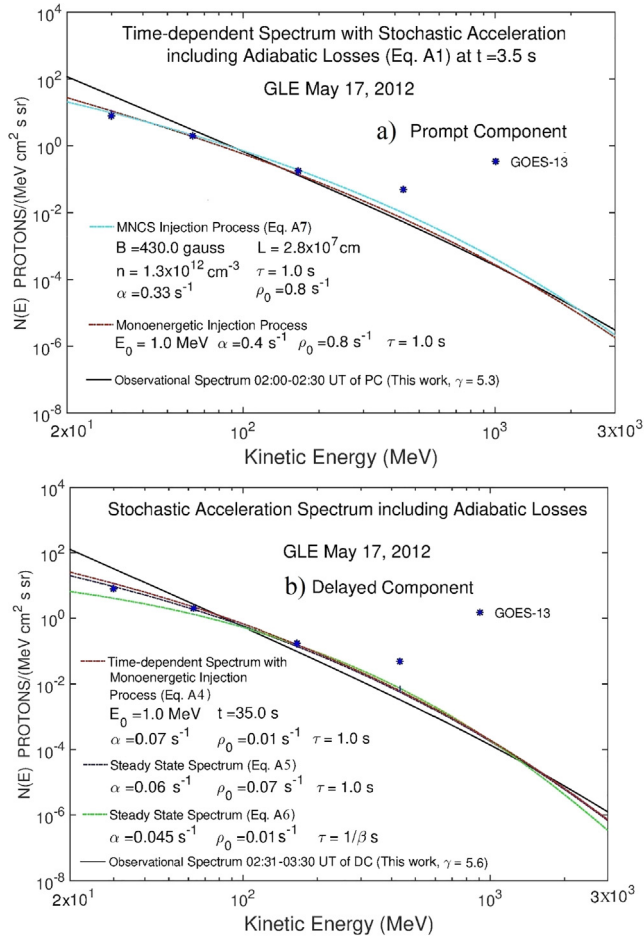
Fig. 8. The comparison of the theoretical spectra to the observational spectra of this work is shown for the GLE of May 17, 2012. Fig. (a) corresponds to the PC of the GLE event and Fig. (b) corresponds to the DC of the same event, when it is reaching the stationary state.

Similarly, Fig. 9a–f show the fitting of our observational Prompt and Delayed spectra illustrated in Fig. 6b. The source parameters for both components of the spectrum are indicated in the body of the Figures.

The corresponding parameters are summarized in Table 2. Column 7 indicates the parameter of the acceleration efficiency of the stochastic process. Column 8 indicates the efficiency of the deceleration process of adiabatic cooling. Column 9 indicates the monoenergetic injection energy to the acceleration process. Column 10 indicates the mean confinement time of particles in the source. Column 11 is the acceleration time of particle, which may be assimilated to the time where the process reaches the steady-state. Column 12 is the average of the magnetic field in the magnetic neutral current sheet (MNCS). Column 13 is the average length of the MNCS. Column 14 is the density number in the source. Column 15 indicates the kind of injection into the acceleration process.

The flare conditions in these two small events are quite similar, in fact, it can be noted that there is not a considerable dispersion of the acceleration efficiency values; turbulence must have been quite similar in regions where the

magnetic field strength is in the range of 400–550 *Gauss* and density in the range 10^{11}–10^{12} cm^{-3}. Also, upon observing column 8 one can infer that the adiabatic deceleration efficiency (ρ_0) in these two small events is in the range of 0.01–0.8 s^{-1}. It should be noted that the accelerated particles escape from the source either with a quasi-constant mean escape time or, with an inverse dependence of their velocities ($1/\beta$).

7. Discussion

The GLE of May 17, 2012, and September 10, 2017, were very peculiar in the sense that they were relatively small, showing a hard spectrum, moving to a softer spectrum as time went by. The May 17, 2012 GLE originated in a flare of class M5.1, occurring at approximately 01:39 UT, with heliolongitude in the range of W20-W90, Li et al., (2013). According to Omodei et al., (2018) the second GLE event was associated with a X8.2 type flare in the solar zone (S08-W83), after 16:30 UT. This increase was also registered for some non-polar stations, but of high latitude.

This paper demonstrates the effectiveness of the method developed to calculate the observational energy spectrum, for the particular case where the involved instruments are at the same location. This allows to determine the spectra parameters J_o and γ during weak events, Caballero-Lopez and Moraal (2016), and we did this here for both phases (PC and DC) of each event, and in this way, we generated the observational spectrum (Fig. 6 and Table 1). We observe in Table 1 that the spectral indexes for the studied GLEs are in the order of $\gamma \approx 5$–6. Also, it should be noted that the spectrum of the second phase (or Delayed Component) is softer than that of the first phase (or Prompt Component). The analysis was performed in the energy range ≤ 3 *GeV*.

As was mentioned in Section 1, the phenomena that take place in the sources of solar energetic particles can be inferred from different standpoints, most of them appealing to the temporal synchronization between the various electromagnetic emissions of flares and coronal mass ejections (CME). Another option is through the study of energetic particles, based on the comparison between the observational and the theoretical spectra. In the work at hand, we try to infer about source phenomena through this last option. This is done by adjusting the observational spectra to our theoretical spectra developed in (Gallegos-Cruz and Perez-Peraza, 1995; Perez-Peraza et al., 2009, Perez-Peraza et al., 2018; Perez-Peraza and Marquez-Adame, 2018) and applied, under the assumptions made of a time-dependent situation and a stationary one. The corresponding spectra developed in Gallegos-Cruz and Perez-Peraza, (1995), are synthesized in the *Appendix*. Such a comparison leads us to infer as to plausible scenarios of particle generation in these two peculiar GLEs (Table 2). In the process of comparison of the theoretical spectra with the observational one, we have employed Eq. (A4), Eq. (A5) and Eq. (A6),
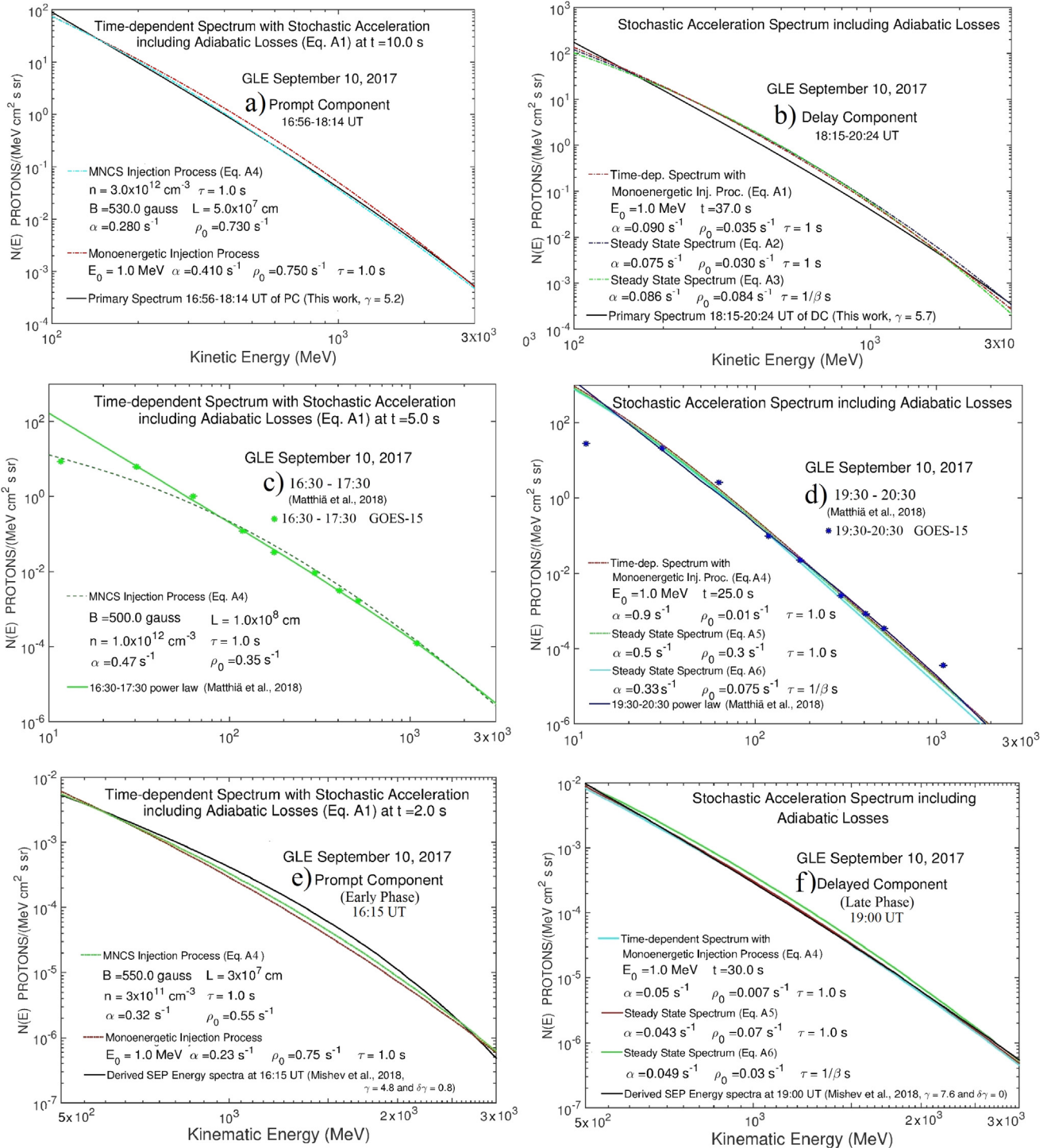
Fig. 9. The comparison of the theoretical spectra to the observational spectra of this work is shown for the GLE of September 10, 2017. Figures a, c and e correspond to the PC of the GLE event, including flux values at low energies from the GOES-13 and GOES-15. Figures b, d and f correspond to the DC of the GLE event.

as well as Eq. (A7), assuming that the stochastic acceleration is preceded by an injection process, either by a local monoenergetic flux of protons of mean energy about 1 MeV, or by an injection from a deterministic process due to the intense electric fields generated in a Magnetic Neutral Current Sheet (MNCS) reconnection process (Perez-Peraza et al., 1978, 2009).

In Figs. 8 and 9 it can be seen that the best fitting Prompt Component phase (PC) of the experimental spectra, occurred when the acceleration is still at a time $t \approx 2$–$10\ s$, whereas for the Delayed Component phase (DC) the best fitting is obtained at $t \geq 25\ s$. It should be noted that the September 10, 2017, Prompt Component (PC) is better described with an injection from a

Table 2
Steady State Stochastic.*

Date GLE	UT	Stage	Spectrum		FIT									Injection	Fig.
			Observational	Theoretical	Eqs.	A (s⁻¹)	ρ0 (s⁻¹)	E₀ (MeV)	T (s⁻¹)	t (s)	B	L	n		
17-May-12	02:00–02:30	PC	This work	Time-Dep. Stoch Accel	(A4)	0.4	0.8	1	1	3.5				Monoenergetic	8a
17-May-12	02:00–02:30	PC	This work	Time-Dep. Stoch Accel	(A4) and (A7)	0.33	0.8	1	1	3.5	430	2.8E+7	1.3E+12	MNCS (Eq. (A7))	8a
17-May-12	02:44–03:30	DC	This work	Time-Dep. Stoch Accel	(A4)	0.07	0.01	1	1	35				Monoenergetic	8b
17-May-12	02:44–03:30	DC	This work	SSS Accel	(A5)	0.06	0.07		1					Monoenergetic	8b
17-May-12	02:44–03:30	DC	This work	SSS Accel	(A6)	0.045	0.01		1/β					Monoenergetic	8b
10-Sep-17	16:56–18:14	PC	This work	Time-Dep. Stoch Accel	(A4)	0.39	0.8	1	1	10				Monoenergetic	9a
10-Sep-17	16:56–18:14	PC	This work	Time-Dep. Stoch Accel	(A4) and (A7)	0.26	0.75	1	1	10	500	1E+8	1E+12	MNCS (Eq. (A7))	9a
10-Sep-17	18:15–20:24	DC	This work	Time-Dep. Stoch Accel	(A4)	0.07	0.04	1	1	37				Monoenergetic	9b
10-Sep-17	18:15–20:24	DC	This work	SSS Accel	(A5)	0.05	0.03		1					Monoenergetic	9b
10-Sep-17	18:15–20:24	DC	This work	SSS Accel	(A6)	0.067	0.093		1/β					Monoenergetic	9b
10-Sep-17	16:30–17:30	PC	Matthiä 2018	Time-Dep. Stoch Accel	(A3) and (A7)	0.47	0.35		1	5	500	1E+8	1E+12	MNCS (Eq. (A7))	9c
10-Sep-17	19:30–20:30	DC	Matthiä 2018	Time-Dep. Stoch Accel	(A4)	0.9	0.01	1	1	25				Monoenergetic	9d
10-Sep-17	19:30–20:30	DC	Matthiä 2018	SSS Accel*	(A5)	0.5	0.3		1					Monoenergetic	9d
10-Sep-17	19:30–20:30	DC	Matthiä 2018	SSS Accel	(A6)	0.33	0.075		1/β					Monoenergetic	9d
10-Sep-17	16:15	PC	Mishev 2018	Time-Dep. Stoch Accel	(A4)	0.23	0.75	1	1	2				Monoenergetic	9e
10-Sep-17	16:15	PC	Mishev 2018	Time-Dep. Stoch Accel	(A4) and (A7)	0.32	0.55	1	1	2	550	3E+7	3E+11	MNCS (Eq. (A7))	9e
10-Sep-17	19:00	DC	Mishev 2018	Time-Dep. Stoch Accel	(A4)	0.05	0.007	1	1	30				Monoenergetic	9f
10-Sep-17	19:00	DC	Mishev 2018	SSS Accel	(A5)	0.043	0.07		1					Monoenergetic	9f
10-Sep-17	19:00	DC	Mishev 2018	SSS Accel	(A6)	0.049	0.03		1/β					Monoenergetic	9f

* The meaning of the symbols is described in the Appendix.

reconnection process; though a monoenergetic injection process cannot be disregarded, since both options reproduce the observational spectrum quite correctly. The Delayed Component (DC) seems to be systematically better described by stochastic acceleration with the injection from a monoenergetic flux. The steady-state situation seems to be reached after a time around 40 s in the source.

Figs. 8 and 9 including data from the GOES-13 and GOES-15 satellite show that, data satellite may be correctly fitted by our theoretical and our experimental spectra. In addition to the authors mentioned in the text, it should be said that no other space detectors have provided public information on proton fluxes during the occurrence of GLE71 and GLE72.

Regarding the physical scenarios, in general, we have found that stochastic acceleration while losing energy by adiabatic losses during the source expansion compares much better to the observational spectra in contrast to the case when adiabatic cooling is ignored. As can be seen in Figs. 8b, 9b, 9d and 9f, the possible scenario at the source of the Delayed Component for both GLEs is better described with a time-dependent spectrum of stochastic acceleration, with a monoenergetic injection and a mean confinement time of ~1 s (Eq. (41) in Ap. J. 446, 1995) by adding losses due to adiabatic cooling; whereas in the Prompt Component, injection from a MNCS is quite probably present as can be observed in Figs. 8a, 9a, 9c and 9e. The corresponding parameters of the source processes are shown in Table 2.

We claim thus that our work leads to construct possible scenarios in the source during the generation of each GLE: throughout the enhanced solar activity of the first days of September 2017, due to magnetic field reconfiguration, strong electric fields were generated together with high levels of turbulence; consequently, solar protons were accelerated either by a primary acceleration mechanism (most probably from reconnection in a MNCS). Alternatively, protons of E ≥ 1 MeV from the high energy tail of the local plasma Maxwell distribution were accelerated by a stochastic process, either in the flare body or in its surroundings, or behind the shock wave.

8. Conclusions

We explored the sources of particles during the GLE of May 12, 2012, and September 10, 2017 based on the observational spectrum developed here. For the GLE of September 10, 2017, we have considered also the spectra given by other authors.

In addition of deriving the observational spectra of both GLEs, the main results of this work to be emphasized are the set of source parameters for the generation of particles and the acceleration processes involved, which lead to plausible scenarios during the events under study. It is precisely the comparison of the theoretical source spectra with the observational spectra that gives us an approximate conception of the production scenarios. The analysis of the

spectra leads us to consider the presence of two different particle components during the events. Some authors designate those two phases as Prompt and Delayed Components, other authors use the terms Early and Late Phases, or even stages. These two components may indicate the occurrence of two acceleration processes of a different nature, as is frequently evoked by many authors. In both phases, the main acceleration mechanism is most probably of stochastic nature, where the particle injection process to the stochastic mechanism can come from a monoenergetic proton flux that may have originated from the high energy tail of the pre-accelerated protons in the MNCS. However, in this work another option is opened: *a single acceleration mechanism in two different acceleration stages* could be generated in a deterministic process with a spectrum like that shown in Eq. (A7), so that a unique stage of acceleration in a MNCS cannot be disregarded. Finally, we emphasize that the comparison between the theoretical and observational spectra gives us an approximate conception of the production scenarios, that is, of the involved processes of acceleration and loss of energy, as well as of the plausible physical parameters that prevail at the source.

Declaration of Competing Interest

Acknowledgement

Appendix. By means of the quasi-linear theory, and introducing the effects of spatial transport in a time escape (Schlickeiser, 1989), a diffusion equation in moment space is obtained from the Vlasov equation (collisionless Boltzmann equation). That can be also derived from the Chapman-Kolmogorov equation (e.g., Schatzman, 1966).

$$\frac{\partial f(p,t)}{\partial t} = \frac{1}{p^2}\frac{\partial}{\partial p}\left[p^2 D(p)\frac{\partial f(p,t)}{\partial p}\right] \qquad (A1)$$

In Eq. (A1) $f(p, t)$ is the pitch angle averaged-density of particles of momentum p interacting with turbulence at time t, and $D(p)$ is the diffusion coefficient characterizing the interaction dynamics between particles and the specific type of turbulence, which is assumed to be homogeneous and time independent (Tsytovich, 1977). Furthermore, an alternative solution for this diffusion equation may be found by its transformation into a Fokker-Planck-type equation in the energy space of particles (Ginzburg and Syrovatskii, 1964), Eq. (A2):

$$\frac{\partial N(E,t)}{\partial t} = \frac{1}{2}\frac{\partial^2}{\partial E^2}[D(E)N(E,t)] - \frac{\partial}{\partial E}[B(E)N(E,t)] \qquad (A2)$$

where E is the particle kinetic energy, and $N(E, t)$ is the number of particles per energy interval at time t, $D(E)$ is the diffusive energy change rate produced by the dispersion in energy gain around the value of the systematic energy gain rate, given by $B(E)$ The effect of systematic energy losses or any other systematic acceleration effect may be introduced in the second term of the right-hand of the previous equation by setting $A(E) = B(E) \pm$ *additional systematic energy change processes* (Ginzburg, 1958). Also, a source term $Q(E, t)$ is added, (indicating external particle injection into the acceleration region) and a sink term, assumed to describe any kind of particle disappearance process from the acceleration volume by means of characteristic disappearance (or scape) time $\tau(E, t)$, employing these arguments, the previous equation is usually rewritten as:

$$\frac{\partial N(E,t)}{\partial t} = \frac{1}{2}\frac{\partial^2}{\partial E^2}[D(E)N(E,t)] - \frac{\partial}{\partial E}[A(E)N(E,t)]$$
$$- \frac{N(E,t)}{\tau(E,t)} + Q(E,t) \qquad (A3)$$

$A(E)$ being the systematic effect of stochastic acceleration and deceleration processes as any eventual secular energy change effect. And $D(E)$ being the diffusive effects due to dispersion around the systematic energy change rate $A(E)$; $D(E)$ was discussed in Perez-Peraza and Gallegos-Cruz (1994). There is not at present an analytical time-dependent solution for the entire particle energy range. Analytical expressions have been only derived in the asymptotic ranges, $E \ll mc^2$ and $E \gg mc^2$ (e.g., Melrose, 1976, 1980; Barbosa 1979; Ramaty 1979). However, the spectrum of protons in the transrelativistic region is very important for the production of neutrons, pions and gamma-nuclear lines in solar flares.

Among the usual simplifications to solve Eq. (A3) are to assume time independence for the escape and injection functions as well as time-independent and energy-independent acceleration efficiency (constant). To avoid some of these simplifications, we herein propose the use of the WKBJ technique to solve the last equation over the complete energy range of the accelerated particles. In mathematical physics, the WKBJ approximation Wentze (1926), Kramer (1926), Brilloui (1926) and Jeffreys (1924)

is a method for finding approximate solutions to linear differential equations with spatially varying coefficients. It is typically used for a semiclassical calculation in <u>quantum mechanics</u> in which the wavefunction is recast as an exponential function, semiclassically expanded, and then either the amplitude or the phase is taken to be changing slowly. Some people designate it as WBK, BWK or JWKB. An authoritative discussion and critical survey has been given by Balson Dingle, (1973) and Kichigin et al. 2019.

Since we have no confident inferences about the time dependence of the injection process, we retain, for simplicity, the general assumption that the flux $N(E, t)$ is being injected at a rate $Q(E) = q(E)\Theta(t) \approx q(E)$ [where $\Theta(t)$ is the step function] and is escaping at a rate τ^{-1}, Gallegos-Cruz and Perez-Peraza (1995).

The theoretical spectra used in this work are:

The Time-dependent Spectrum for MHD turbulence, with monoenergetic injection, $\tau = cst$, and $D(p) = p^2/\beta$ has been given in the Eq. (41) in Gallegos-Cruz and Perez-Peraza (1995), Eq. (3) in Perez-Peraza et al. (2009): this formulation with the incorporation of adiabatic energy losses was employed in Perez-Peraza et al. (2018) and the inclusion of collisional energy losses will appear soon.:

$$N(E,t) \cong \frac{(\beta_0/\beta)^{1/4}(\varepsilon/\varepsilon_0)^{1/2}\left(\beta_0^{3/2}\varepsilon_0\right)^{-1}}{\left(\frac{4\pi\alpha}{3}\right)^{1/2}}$$
$$\times \left[\left(\frac{N_0}{t^{1/2}}\right)exp\left(-a_f t - \frac{3J_f^2}{4\alpha t}\right) + \left(\frac{q_0}{2}\right)\left(\frac{\pi}{a_f}\right)^{\frac{1}{2}}R_5(\varepsilon_0,\varepsilon)\right]$$
$$\times F(\rho_0) \text{ protons/(MeV s cm}^2 \text{ str)} \qquad (A4)$$

where $\left(\frac{dE}{dt}\right)_{acc} = \alpha\beta E$ (MeV/s) = the stochastic acceleration rate; and $\left(\frac{dE}{dt}\right)_{ad} = -\rho_0\beta^2 E$ (MeV/s) = deceleration rate,

With $\alpha(s^{-1})$ the acceleration efficiency and $\rho_0 = (2/3)(V_r/R)(s^{-1})$ is the deceleration efficiency due to adiabatic cooling. Furthermore V_r and R are the expanding velocity and linear extension of the expanding magnetic structure respectively; $N_0 = protons/4\pi R_{SE}^2$; $q_0 = protons/4\pi R_{SE}^2 s$ and $R_{SE} = 1.5 \times 10^{13}$ cm = sun-earth distance.

$$R_5(\varepsilon_0,\varepsilon) = [erf(Z_1) - 1]exp\left[\left(3a_f/2\alpha\right)J_f^2\right]$$
$$+ [erf(Z_2) + 1]exp\left[-\left(3a_f/2\alpha\right)J_f^2\right]$$

$$Z_{1,2} = (a_f t)^{1/2} \pm (3a_f/4\alpha t)^{1/2}J_f;$$

$$a_f = \left(\frac{\alpha}{3}\right)\left(\bar{F} + \frac{3}{\alpha\tau} - 3\rho(4 - \beta^2 - \beta_0^2)/2\alpha\right);$$

$$\bar{F} = 0.5\left[\beta^{-1} + 3\beta - 2\beta^3 + \beta_0^{-1} + 3\beta_0 - 2\beta_0^3\right];$$

$$\beta = (\varepsilon^2 - m^2c^4)^{1/2}/\varepsilon; \quad \beta_0 = (\varepsilon_0^2 - m^2c^4)^{1/2}/\varepsilon_0$$

$$J_f = tan^{-1}\beta^{\frac{1}{2}} - tan^{-1}\beta_0^{1/2} + 0.5ln\left[\frac{\left(1 + \beta^{1/2}\right)\left(1 - \beta_0^{1/2}\right)}{\left(1 - \beta^{1/2}\right)\left(1 + \beta_0^{1/2}\right)}\right];$$

$$F(\rho_0) = \left[\frac{\varepsilon_0(1+\beta_0)}{\varepsilon(1+\beta)}\right]^{3\rho_0/2\alpha} \text{ With } \varepsilon_0 \text{ the injection energy (MeV)}$$

The Steady-State Spectrum for MHD turbulence, monoenergetic injection, $\tau = cst.$, and $D(p) = p^2/\beta$, has been given in the Eq. (42) in Gallegos-Cruz and Perez-Peraza (1995): this formulation was also developed with the inclusion of adiabatic energy losses:

$$N(E) \approx (q_0/2)(a_f\alpha/3)^{-1/2}\left(\beta_0^{3/2}\varepsilon_0\right)^{-1}(\beta_0/\beta)^{1/4}(\varepsilon/\varepsilon_0)^{1/2}$$
$$\times exp\left[-\left(3a_f/\alpha\right)^{1/2}J_f\right]\left[\frac{F(\rho_0)}{4\pi R_{SE}^2}\right] \text{ protons/(MeV cm}^2 \text{ str)}$$
$$\qquad (A5)$$

Where: $\alpha, \rho_0, a_f, \bar{F}, J_f, \beta, \beta_0, \varepsilon_0, F(\rho_0)$ and R_{SE} are the same as in Eq. (A4).

The Steady State Spectrum for MHD turbulence, monoenergetic injection, $\tau \approx 1/\beta$, and $D(p) \approx p^2/\beta$, has been given in the Eq. (43) in Gallegos-Cruz and Perez-Peraza (1995): this formulation with the incorporation of adiabatic energy losses was employed in Perez-Peraza et al. (2018):

$$N(E) = \frac{(q_0/2)(\beta_0/\beta)^{\frac{1}{4}}(\varepsilon/\varepsilon_0)^{\frac{1}{2}}}{(4\pi R_{SE}^2)(\alpha/3)^{\frac{1}{2}}a^{\frac{1}{4}}(E)a^{\frac{1}{4}}(E_0)\beta_0^{\frac{3}{2}}\varepsilon_0}\left[\frac{\varepsilon + \beta\varepsilon}{\varepsilon_0 + \beta_0\varepsilon_0}\right]^{-\left(b+\frac{1}{2b}\right)}$$
$$\times exp\left[\left(\frac{-1}{2b}\right)\left(\beta^{-1} - \beta_0^{-1}\right)\right]F(\rho_0) \text{ protons/(MeV cm}^2 \text{ str)}$$
$$\qquad (A6)$$

where: $\alpha, \rho_0, a_f, \bar{F}, J_f, \beta, \beta_0, \varepsilon_0, F(\rho_0)$ and RSE are the same as in Eq. (A4).

The Steady-State Spectrum of acceleration by a Direct Electric Field in a Magnetic Neutral Current Sheet (MNCS), has been given in Perez-Peraza et al., (1978) and Eq. (1) in Perez-Peraza eta al. (2009):

$$N(E) = N_0(E/E_c)^{-\frac{1}{4}}exp\left[-1.12(E/E_c)^{3/4}\right] \text{ protons/(MeV cm}^2 \text{ str)}$$
$$\qquad (A7)$$

With $N_0 = 8.25 \times 10^5\left(\frac{nL^2}{B}\right)\left(\frac{1}{E_c}\right)/4\pi R_{SE}^2$ protons/(MeV cm² str), assuming anomalous conductivity; $E_c = 1.792 \times 10^3\left(\frac{B^2L}{n}\right)$ MeV, B = magnetic field strength (gauss), L = length of the MNCS (cm); and n = plasma number density (cm⁻³).

References

Álvarez, M., Miroshnichenko, L.I., Perez-Peraza, J., Rivero-G, F., 1986. Spectrum of solar cosmic rays in the source taking into account their coronal propagation. Soviet Astr. 66, 1169–1181.

Augusto, C.R.A., Kopenkin, V., Navia, C.E., Felicio, A.C.S., Freire, F., Pinto, A.C.S., 2013. Was the GLE on May 17, 2012 linked with the M5.1-class flare the first in the 24th solar cycle? arXiv:1301.7055, Astroph. SR. p. 1–9.

Augusto, C.R.A., Navia, C.E., de Oliveira, M.N., Nepomuceno, A.A., Fauth, A.C., Kopenkin, V., Sinzi, T., 2018. Relativistic proton levels from region AR2673 (GLE #72) and the heliospheric current sheet as a Sun-Earth magnetic connection. Preprint of the Alamos Laboratory, arXiv:1805.02678v1 [astro-ph.SR].

Balabin, Y.V., Germanenko, A.V., Gvozdevsky, B.B., Vashenyuk, E.V., 2015. Analysis of the Event GLE72 of 6 January 2014. J. Russian Acad. Sci. Ser. Phys. 79 (5), 612–614. https://doi.org/10.7868/S0367676515050099.

Barbosa, D.D., 1979. Stochastic acceleration of solar flare protons. ApJ 233, 383–394. https://doi.org/10.1086/157399.

Balabin, Yu.V., Germanenko, A.V., Vashenyuk, E.V., Gvozdevsky, B.B., 2013. The first GLE of the new 24th solar cycle. In: Proceedings 33rd International Cosmic Ray Conference, Rio de Janeiro, Brazil, 1, p. 1467–1470.

Balson Dingle, R., 1973. Asymptotic Expansions: Their Derivation and Interpretation. Academic Press, London.

Berrilli, F., Casolino, M., Del Moro, D., Di Fino, L., Larosa, M., Narici, L., Piazzesi, R., Picozza, P., Scardigli, S., Sparvoli, R., Stangalini, M., Zaconte, V., 2014. The relativistic solar particle event of May 17th, 2012 observed on board the International Space Station. Weather Space Clim. 4 (A16), 1–8. https://doi.org/10.1051/swsc/2014014.

Bieber, J.W., Evenson, P., 1991. Determination of energy spectra for the large solar particle events of 1989. In: Proceedings 22nd International Cosmic Ray Conference, Dublin, 3, p. 129–133.

Bieber, J.W., Dröge, W., Evenson, P.A., Pyle, R., Ruffolo, D., Pinsook, U., Tooprakai, P., Ujiwarodom, M., Khumlumlert, T., Krucker, S., 2002. Energetic particle observations during the 2000 July 14 solar event. ApJ 567, 622–634.

Brillouin, Léon, 1926. La mécanique ondulatoire de Schrödinger: une méthode générale de resolution par approximations successives The wave mechanics of Schrödinger: a general method of successive approximation solving. Comptes Rendus de l'Académie des Sciences 183, 24–26.

Bieber, J.W., Clem, J., Evenson, P., Pyle, R., Sáiz, A., Ruffolo, D., 2013. Giant ground level enhancement of relativistic solar protons on 2005 January 20.I. Spaceship earth observations. ApJ, 771–792.

Caballero-Lopez, R.A., Moraal, H., 2012. Cosmic-ray yield and response functions in the atmosphere. J. Geophys. Res. 117, A12103, 1–11. https://doi.org/10.1029/2012JA017794.

Caballero-Lopez, R.A., Moraal, H., 2016. Spectral index of solar cosmic-ray flux from the analysis of ground-level Enhancements. Adv. Space Res. 57, 1314–1318.

Cohen, C.M.S., Mewaldt, R.A., 2018. The ground-level enhancement event of September 2017 and other large solar energetic particle events of cycle 24. Space Weather 16 (10), 1616–1623. https://doi.org/10.1029/2018SW002006.

De Koning, C.A., 1994. Significant proton events of solar cycle 22 and a comparison with events of previous solar cycles Thesis. University of Calgary.

Dorman, L.I., Venkatesan, D., 1993. Solar cosmic rays. Space Sci. Rev. 64, 183–362, Doi: 1993SSRv..64..183D.

Forman, M.A., Ramaty, R., Zweibel, E.G., et al., 1986. In: Physics of the Sun. D. Reidel Publishing Company, Dordrecht, Holland, pp. 249–324, Chapter13.

Gallegos-C, A., Perez-Peraza, J., 1987. Determination of energy spectra of solar electrons under different scenarios in solar flare sources. Rev. Mexicana Astron. Astrof. 14, 700–704.

Gallegos-C, A., Perez-Peraza, J., Miroshnichenko, L.I., Vashenyuk, E.V., 1993. Solar particle acceleration by slow magnetosonic waves. Adv. Space. Res. 13 (9), 187–190.

Gallegos-Cruz, A., Perez-Peraza, J., 1995. Derivation of analytical particle spectra from the solution of the transport equation by the WKBJ method. Astrophys. J. 446, 400–420.

Ginzburg, V.L., 1958. Progress in Elementary Particle and Cosmic Ray Physics, Vol. 4. Elsevier, Amsterdam.

Ginzburg, V.L., Syrovatskii, S.I., 1964. Origin of Cosmic Rays. Pergamon Press, Oxford.

Gopalswamy, N., Xie, H., Akiyama, S., Yashiro, S., Usoskin, I.G., Davila, J.M., 2013. The first ground level enhancement event of solar cycle 24: direct observation of shock formation and particle release heights. Ap. J. Letters. 765:L30. https://doi.org/10.1088/2041-8205/765/2/L30, p. 1–38 5.

Gopalswamy, N., Yashiro, S., Makel1, P., Xie, H., Akiyama, S., Monstein, C., 2018. Extreme kinematics of the 2017 September 10 solar eruption and the spectral characteristics of the associated energetic particles. ApJ 863 (L39), 1–6, https://iopscience.iop.org/article/10.3847/2041-8213/aad86c.

Harold, Jeffreys, 1924. On certain approximate solutions of linear differential equations of the second order. Proc. London Math. Soc. 23, 428–436. https://doi.org/10.1112/plms/s2-23.1.428.

Kichigin, G.N., Kravtsova, M.V., Sdobnov, V.E., 2019. Global solar magnetic field and cosmic ray ground level enhancement. Solar Phys. 294 (116), 1–10. https://doi.org/10.1007/s11207-019-1516-5.

Kramers, H.A., 1926. Wellenmechanik und halbzahlige Quantisierung. Z. Physik 39 (10-11), 828–840. https://doi.org/10.1007/BF01451751.

Kuwabara, T., Bieber, J., Clem, J., Evenson, P., Gaisser, T., Pyle, R., Tilav, S., 2012. Ground Level Enhancement of May 17, 2012, Observed at South Pole. In: 45th AGU Fall Meeting, SH21A-2183 (Poster), San Francisco.

Kuwabara, T., Bieber, John, Clem, John, Evenson, Paul, Gaisser, Tom, Pyle Serap Tilav, Rogert, 2013: The Ice Cube Collaboration, 2013: Ground Level Enhancement of May 17, 2012 Observed at South Pole. In: Proc. 33rd ICRC, RIO DE JANEIRO 2013; The Astroparticle Physics Conference (See Special Section of these Proceedings), p. 1347–1350.

Li, C., Kazi, A., Firoz, L., Sun, P., Miroshnichenko, L.I., 2013. Electron and proton acceleration during the first ground level enhancement event of solar cycle 24. ApJ 770(1) (34), 1–11.

Matthiä, Daniel, Meier, Matthias M., Berger, Thomas, 2018. The solar particle event on 10-13 September 2017: spectral reconstruction and calculation of the radiation exposure in aviation and space. Space Weather 16 (8), 977–986. https://doi.org/10.1029/2018SW001921.

McCracken, K.G., Moraal, H., Shea, M.A., 2012. The high-energy impulsive ground-level enhancement. ApJ. 761 (101), 1–12. https://doi.org/10.1088/0004-637X/761/2/101.

Melrose, D.B., 1976. Precipitation in trap models for solar hard X-ray bursts. MNRAS 176 (1), 15–30. https://doi.org/10.1093/mnras/176.1.15.

Miroshnichenko, L.I., 2001. In: Solar Cosmic Rays. Kluwer Academic Publisher, The Netherlands, Astrophysics and Space Science Library, V. 260, p. 480.

Miroshnichenko, L.I., Perez-Peraza, J., 2008. Astrophysical Aspects in the studies of solar cosmic rays (Invited Article). Int. J. Modern Phys. A 23 (1), 1–14.

Miroshnichenko, L.I., 2014. Solar Cosmic Rays: Fundamentals and Applications, second ed. Springer, Berlin, p. 521.

Mishev, A.L., Kocharov, L.G., Usokin, I.G., 2014. Analysis of the ground level enhancement on 17 May 2012 using data fromthe global neutron monitor network. J. Geophys. Res. Space Phys. 119, 670–679. https://doi.org/10.1002/2013JA019253.

Mishev, A., Usoskin, I., Raukunen, O., Paassilta, M., Valtonen, E., Kocharov, L., Vainio, R., 2018. First analysis of ground-level enhancement (GLE) 72 on 10 September 2017: spectral and anisotropy characteristics. Sol. Phys. 293 (136), 1–15.

Moraal, H., Caballero-Lopez, R.A., 2014. The cosmic-ray ground-level enhancement of 1989 September 29. ApJ 790 (2), 154. https://doi.org/10.1088/0004-637X/790/2/154.

Oh, S.Y., Bieber, J.W., Clem, J., Evenson, P., Pyle, R., Yi, Y., Kim, Y.K., 2012. South Pole neutron monitor forecasting of solar proton radiation intensity. Space Weather S05004, 1–13. https://doi.org/10.1029/2012SW000795.

Omodei N., Pesce-Rollins M., Longo F., Allafort A., Krucker S., 2018. Fermi-LAT observations of the 2017 September 10th solar flare Preprint of the Alamos Laboratory. arXiv: 1803.07654v1 [astro-ph. HE], p. 1–6; DOI: 10.3847/2041-8213/aae077.

Papaioannou, A., Souvatzoglou, G., Paschalis, P., Gerontidou, M., Mavromichalaki, H., 2014. The first ground-level enhancement of solar cycle 24 on 17 May 2012 and its real-time detection. Sol. Phys. 289, 423–436. https://doi.org/10.1007/s11207-013-0336-2.

Perez-Peraza, J., Gálvez, M., Lara-Alvarez, R., 1977. Energy spectrum of flare particles from an impulsive acceleration process. In: Proceedings of the International Cosmic Ray Conference, XV-Vol. 5, p. 23–28.

Perez-Peraza, J., Gálvez, M., Lara-Alvarez, R., 1978. The primary spectrum of suprathermal solar particles. Adv. Space Res. 18, 365–368.

Perez-Peraza, J., Miroshnichenko, L.I., Rivero, F., Álvarez, M., 1985, Source energy spectra from demodulation of solar particle data by interplanetary and coronal transport. In: Proceedings of the International Cosmic Ray Conference, XIX-Vol. 4, p. 110–113.

Perez-Peraza, J.y., Gallegos, A.C., 1987. Solutions of the Fokker-Planck equation for the energy distribution of suprathermal electrons. Rev. Mexicana Astron. Astrof. 14, 705–714.

Perez-Peraza, J., Miroshnichenko, L.I., Sorokin, O.M., Vashenyuk, E.V., Gallegos-C, A., 1993. Spectrum of the fast solar proton component. Geomagnet. Aeronomy 32 (2), 1–12, 1992 (Russian version, p. 159–171).

Perez-Peraza, J., Gallegos-Cruz, A., 1994. Weightiness of the dispersive rate in stochastic acceleration processes. Astrophys. J. Suppl. Ser. 90, 669–682. https://doi.org/10.1017/S0252921100077940.

Perez-Peraza, J., Vashenuyk, E.V., Balabin, Yu.V., Miroshnichenko, L.I., Gallegos Cruz, A., 2009. Impulsive, stochastoc, and shock wave acceleration of relativistic protons in large solar events of 1989 September 29, 2000 July 14, 2003 October 28, and 2005 January 20. ApJ 695, 865–873. https://doi.org/10.1088/0004-637X/695/2/865.

Pérez-Peraza, Jorge, Márquez-Adame, Juan C., Miroshnichenko, Leonty, Velasco-Herrera, Victor, 2018. Source energy spectrum of the 17 May 2012 GLE. J. Geophys. Res. Space Phys. 123 (5), 3262–3272. https://doi.org/10.1002/2017JA025030.

Perez-Peraza, Jorge, Márquez-Adame, Juan C., 2018. Exploration of solar cosmic ray sources by means of particle energy spectra. In: Szadkowski, Zbigniew (Ed.), Cosmic Rays. InTechOpen, London. https://doi.org/10.5772/intechopen.77052, ISBN:978-1-78923-593-7, ISBN: 987-953-51-6247-6.

Plainaki, C., Mavromichalaki, H., Laurenza, M., Gerontidou, M., Kanellakopoulos, A., Storini, M., 2014. The ground-level enhancement of 2012 May 17: derivation of solar proton event properties through the application of the NMBANGLE PPOLA mode. Astrophys. J. 785 (160), 1–12. https://doi.org/10.1088/0004-637X/785/2/160.

Poluianov, S.V., Usoskin, I.G., Mishev, A.L., Shea, M.A., Smart, D.F., 2017. GLE and sub-GLE redefinition in the light of high-altitude polar neutron monitors. Sol. Phys. 292 (176), 1–7. https://doi.org/10.1007/s11207-017-1202-4.

Ramaty, R., 1979. Energetic particles in solar flares, in Particle acceleration mechanisms in astrophysics. In: Arons, J., Max, C., McKee, C.

(Eds.), AIP Conf. Proceedings, 56. American Institute of Physics, New York, pp. 135–154.

Reames, D.V., 1999. Particle Acceleration at the Sun and in the Heliosphere. Space Sci. Rev. V. 90 (34), 413–491. https://doi.org/10.1023/A:I100510583.

Ruffolo, D., Tooprakai, P., Rujiwarodom, M., Khumlumlert, T., Wechakama, M., Bieber, J.W., Evenson, P., Pyle, R., 2006. Relativistic solar protons on 1989 October 22: injection and transport along both legs of a closed interplanetary magnetic loop. ApJ 639, 1186–1205. https://doi.org/10.1086/499419.

Sakurai, K., 1974. Physics of Solar Cosmic Rays. University of Tokyo Press, Tokyo, UTP 22 3402, 68026-5149, ISBN 0-86008-105-2.

Schatzman, E., 1966. Summer School of Theoretical Phys. Les Hooches. Gordon & Breach, New York.

Shea, M.A., Smart, D.F. Wada, M., Inoue, A., 1985. A suggested standardized format for cosmic ray ground-level event data. In: Proceedings of 19th International Cosmic Ray Conference, La Jolla, 5, p. 510–520.

Shea, M.A., Smart, D.F., Adams, J.H., Chennette, D., Feyman, J., Hamilton, D.C., Heckman, G., Konradi, A., Lee, M.A., Nachtwey, D. S., Roelof, E.C., 1988. Toward a descriptive model of solar particle in the heliosphere; Interplanetary particle environment. JPL Publication, 1–13, N89–28455.

Schlickeiser, R., 1989. Cosmic-ray transport and acceleration. I. Derivation of the kinetic equation and application to cosmic rays in static cold media. ApJ 336 (243), 243–293. https://doi.org/10.1086/167009.

Smart, D.F., Shea, M.A., 1993. Predicting and modeling solar flare generate proton fluxes in the inner heliosphere. In: Swemberg (Ed.), Biological Effects and Physics of Solar and Galactic Cosmic Radiation, Part B. Plenum Press, New York, pp. 101–117.

Smart, D.F., Shea, M.A., 2005. A review of geomagnetic cutoff rigidities for earth-orbiting spacecraft. Adv. Space Res. 36, 2012–2020. https://doi.org/10.1016/j.asr.2004.09.015.

Stoker, P.H., 1985. Spectra of solar proton ground level 1 events using neutron monitor and neutron moderated detector recordings. In: Proceedings 19th International Cosmic Ray Conference, La Jolla, Vol. 4, p. 114–117.

Tsytovich, V.N., 1977. Theory of Turbulent Plasma. Consultants Bureau, New York.

Vashenyuk, E.V., Miroshnichenko, L.I., Sorokin, M.O., Perez-Peraza, J. y., Gallegos-Cruz, A., 1993. Search for peculiarities of proton events in solar cycle 22 by ground observation data. Geomagnet. Aeronomy 33 (5), 1–10.

Vashenyuk, E.V., Miroshnichenko, L.I., Sorokin, M.o., Perez-Peraza, J., Gallegos, A., 1994. Large ground level events in solar cycle 22 and some peculiarities of relativistic proton acceleration. Adv. Space Ress. 14 (10), 711–716.

Vashenyuk, E.V., Balabin, Yu. V., Gvozdevsky, B.B., 001. Features of relativistic solar proton spectra derived from ground level enhancement events (GLE) modeling. Astrophys. Space Sci. Trans. 7 (4), 459–463. https://doi.org/10.5194/astra-7-459-2011.

Wentze, L. Gregor, 1926. A generalization of the quantum conditions for the purposes of wave mechanics (Eine Verallgemeinerung der Quantenbedingungen für die Zwecke der Wellenmechanik). Zeitschrift für Physik, 38(6–7), p. 518–529. Bibcode:1926 ZPhy 38.518W. Doi:10.1007/BF01397171

Zhao, M.-X., Le, G.-M., Chi, Y.-T., 2018. Investigation of the possible source for solar energetic particle event of 2017 September 10, RAA (Research in Astronomy and Astrophysics)-2018-0009, p. 1-13, arXiv:1805.01082v1 [astro-ph.SR] 3 May 2018.